Electronic Supplementary Material (ESI) for Materials Horizons.

Controllable co-assembly of organic micro/nano heterostructures from fluorescent and phosphorescent molecules for dual anti-counterfeiting

Chunchen Yang[a], Long Gu[a], Chaoqun Ma[a], Mingxing Gu[a], Xiaoji Xie[a], Huifang Shi[a], Huili Ma[a], Wei Yao[,a], Zhongfu An*[,a], and Wei Huang*[,a,b,]*

[a]Key Laboratory of Flexible Electronics (KLOFE) & Institute of Advanced Materials (IAM) Nanjing Tech University (NanjingTech), 30 South Puzhu Road, Nanjing 211816, China

[b]Shaanxi Institute of Flexible Electronics (SIFE) Northwestern Polytechnical University (NPU), 127 West Youyi Road, Xi'an 710072, China

*E-mail: iamwyao@njtech.edu.cn; iamzfan@njtech.edu.cn; iamwhuang@njtech.edu.cn

Contents

1. Experimental Section

Materials

9, 10- Bis(phenylethynyl)anthracene (BPEA) was purchased from Sigma-Aldrich; and 9-(4,6-Dimethoxy-1,3,5-triazin-2-yl)-9H-carbazole (MCzT) was synthesized by ourselves according to the previous literature. The tetrahydrofuran (THF), N N-Dimethylformamide (DMF) and ethanol (EtOH) were purchased from commercial sources without further treatment.

Preparation of the nanostructures

BPEA nanowires, MCzT nanowires and MCzT nanosheets: In a typical preparation of BPEA nanowires, 100 μL DMF were added into 1 mL BPEA (2 mM) in THF. Then, we dropped 20 μL of mixed solution onto cleaned glass, which was placed in a sealed petri dish. The evaporation of the mixed solvent induced the self-assembly of BPEA molecules. Finally, 1D BPEA nanowires were obtained on the glass after two hours. Similarly, we prepared two types of MCzT nanostructures using a solvent evaporation method. When added 100 μL DMF and 50 μL EtOH into 1 mL MCzT (2 mM) in THF, we obtained 1D MCzT nanowires. In contrast, 2D MCzT nanosheets could be constructed if 50 μL DMF and 100 μL EtOH were added into 1 mL MCzT solution.

M-BNwHs and B-BNwHs: The two kinds of branched heterostructures were prepared via a solvent evaporation induced cooperative self-assembly method. Firstly, 100 μL DMF and 50 μL EtOH were added into 1 mL mixed stocked solution of BPEA (0.2 mM) and MCzT (0.8 mM) in THF (C_{BPEA}/C_{MCzT} = 1:4). Then, 20 μL of the mixed solution was dropped onto cleaned glass placed in a sealed petri dish. Finally, M-BNwHs were obtained on the glass after two hours. B-BNwHs could be obtained when we added 50 μL DMF and 100 μL EtOH into 1 mL mixed solution of BPEA (0.67 mM) and MCzT (0.33 mM) in THF (C_{BPEA}/C_{MCzT} = 2:1).

Measurements

Steady-state fluorescence/phosphorescence spectra were measured using HITACHI F-4600. The phosphorescence spectra were collected with a delay time of 5 ms. The lifetimes and time-resolved emission spectra were carried out on Edinburgh FLSP920 fluorescence spectrophotometer equipped with a xenon arc lamp (Xe 900) and microsecond flash-lamp (μF900), respectively. Photoluminescence quantum efficiency was collected on a Hamamatsu Absolute PL Quantum Yield Spectrometer C11347 under ambient condition. SEM images were obtained by a (JSM-7800F) scanning electron microscopy (SEM). TEM and SAED images were obtained by a (JSM-1400PLUS) transmission electron microscopy. Fluorescence images were recorded using a Nikon DS-Ri2 Microscope Camera. The black-whilte fluorescence images were recorded using an ANDOR ZyLA aCMOS Camera. The excitation source is a mercury lamp (Nikon INTENSILIGHT C-HGFI) equipped with a band-pass filter (330-380 nm for UV light, 510-560 nm for green light).

2. Photophysical properties of BPEA and MCzT crystals.

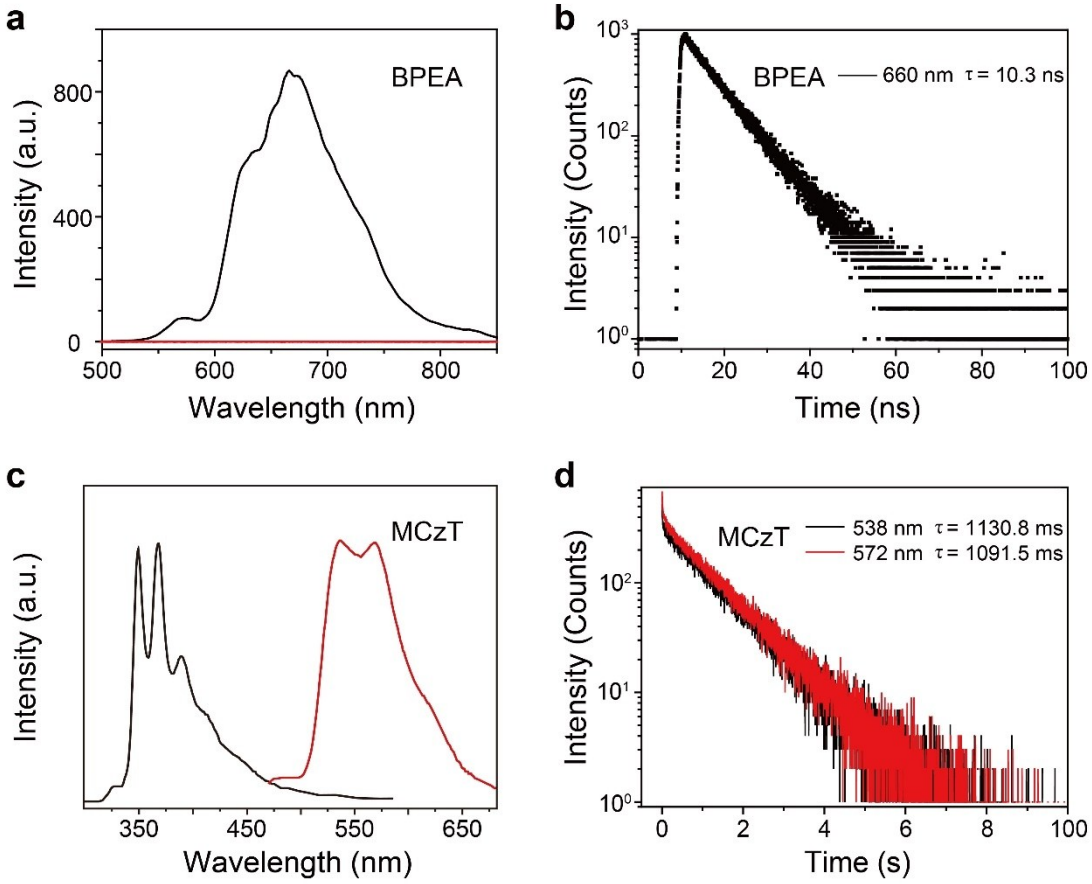

Figure S1. (a) The Steady-state photoluminescence (black line) and phosphorescence spectra (red line) of BPEA crystals excited by 365 nm light. (b) Lifetime decay profiles of the emission band around 665 nm of BPEA crystal. (c) The Steady-state photoluminescence (black line) spectrum of MCzT crystals excited by 315 nm light and phosphorescence spectrum (red line) of MCzT crystals excited by 365 nm light. (d) Lifetime decay profiles of the emission bands around 538 nm and 572 nm of MCzT crystals.

3. The persistent luminescence of MCzT nanostructures.

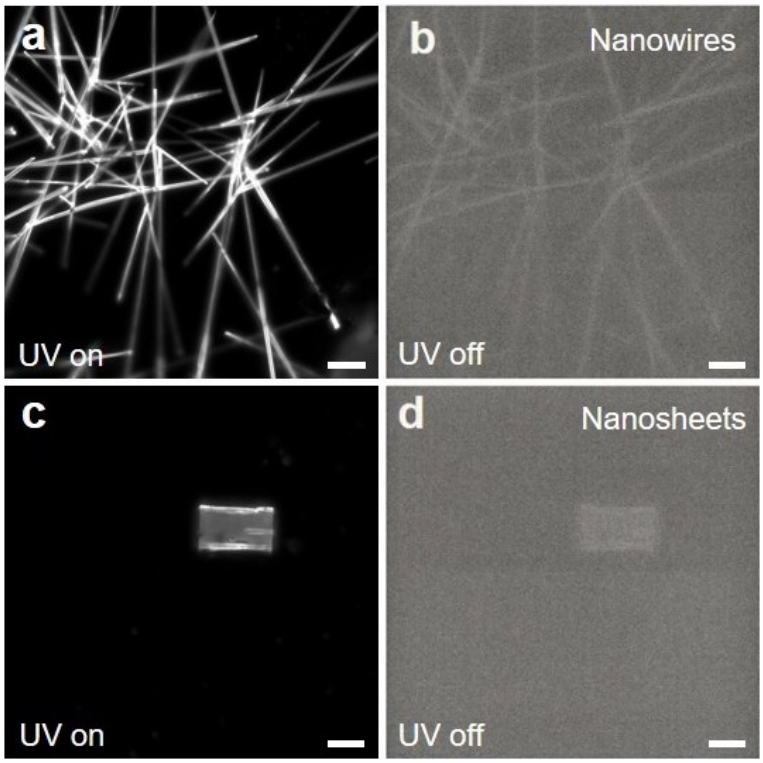

Figure S2. The black-white fluorescence micrography images of MCzT nanostructures under UV on and off. (a, c) The black-white fluorescence micrography images of (a) 1D MCzT nanowires and (c) 2D MCzT nanosheet under unfocused UV light (330-380 nm). (b, d) The micrograph of (b) MCzT nanowires and (d) MCzT nanosheet taken at 0.5 s after turning off the excitation. The scale bar is 10 μm.

4. Fluorescence micrography images of BPEA and MCzT heterostructures prepared under different conditions.

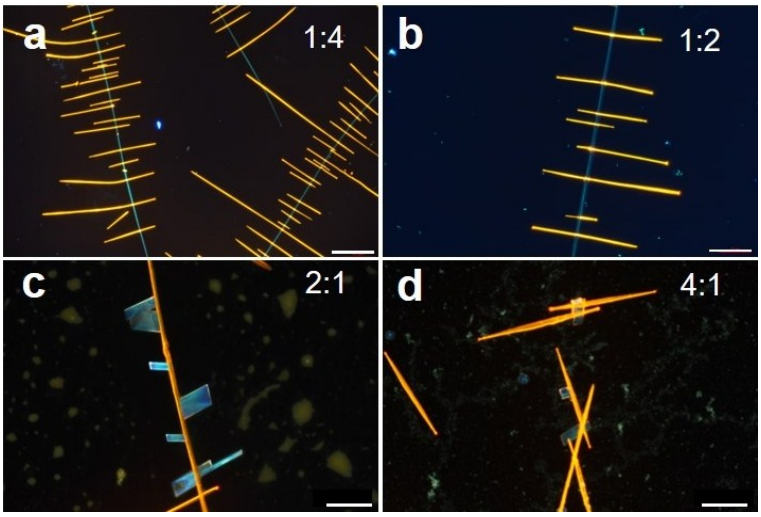

Figure S3. Fluorescence micrography images of organic micro heterostructures prepared at different BPEA/MCzT concentration ratios of (a) 1:4, (b) 1:2, (c) 2:1, (d) 4:1. The fluorescence microscopy images of the nanostructures were excited with UV light (330-380 nm). The (a, d) scale bars are 25 μm. The scale bars of (b, c) are 25 μm.

5. Fluorescence micrography images of organic heterostructures prepared in different concentration and solvent.

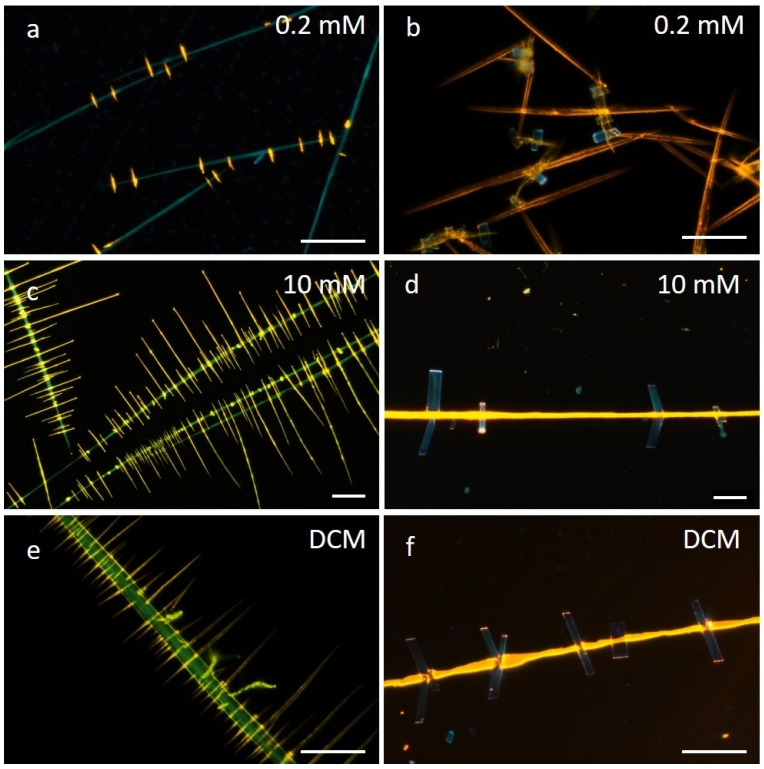

Figure S4. The fluorescent micrographs of organic heterostructures in different preparation conditions. (a, b) The fluorescent micrographs of M-BNwHs (a) and B-BNwHs (b) prepared with 0.2 mM concentration of BPEA and MCzT in THF. The fluorescent micrographs of M-BNwHs (c) and B-BNwHs (d) prepared with 10 mM concentration of BPEA and MCzT in THF. The fluorescent micrographs of M-BNwHs (e) and B-BNwHs (f) prepared by 2 mM concentration of BPEA and MCzT in DCM. The scale bar is 10 μm.

6. The stability of organic heterostructures.

The experiments on stability (photo-, thermal, air-) of the organic heterostructures were carried out under different conditions, which were shown in **Figure S5, S6 S7, S8 and S9**. From **Figure S5 and S6**, we found that the emission intensity of two types of heterostructures (B-BNwHs and M-BNwHs) increased with the power of excitation source increasing. The structure and luminescence of heterostructures did not show any change after irradiated for 30 minutes by UV light (6.55 W/cm^2) (**Figure S5f and S6f**). Impressively, the organic heterostructures kept stable in morphology and photoluminescence after exposing to air for half a year (**Figure S7**). To explore the thermal stability of organic heterostructures, their micrographs at different temperatures were collected (**Figure S8 and S9**). When the temperature was up to 115 ^{o}C, the structure of organic heterostructures were damaged, due to the decomposition of MCzT nanostructures (**Figure S8e and S9e**). These results suggested that the organic heterostructures have good photo- and air- stability, but poor thermal stability.

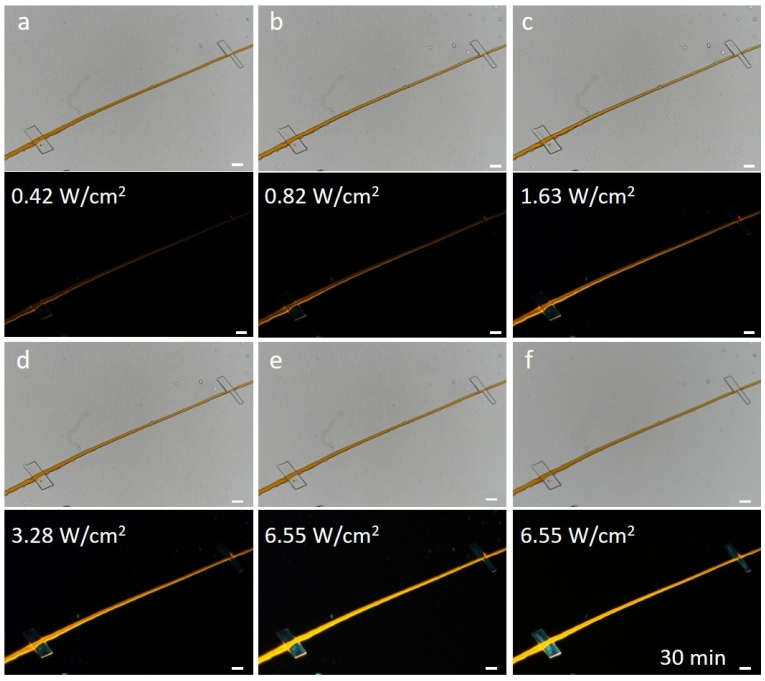

Figure S5. The stability of the B-BNwH under UV light (330-380 nm) irradiation with different power. (a-e) The bright field and fluorescent micrographs of B-BNwH irradiated by a UV excitation source with power of (a) 0.42 W/cm^2, (b) 0.82 W/cm^2, (c) 1.63 W/cm^2, (d) 3.28 W/cm^2 and (e) 6.55 W/cm^2, respectively. (f) The bright field and fluorescent micrographs of B-BNwH irradiated by light source with power of 6.55 W/cm^2 for 30 minutes. The scale bar is 10 μm.

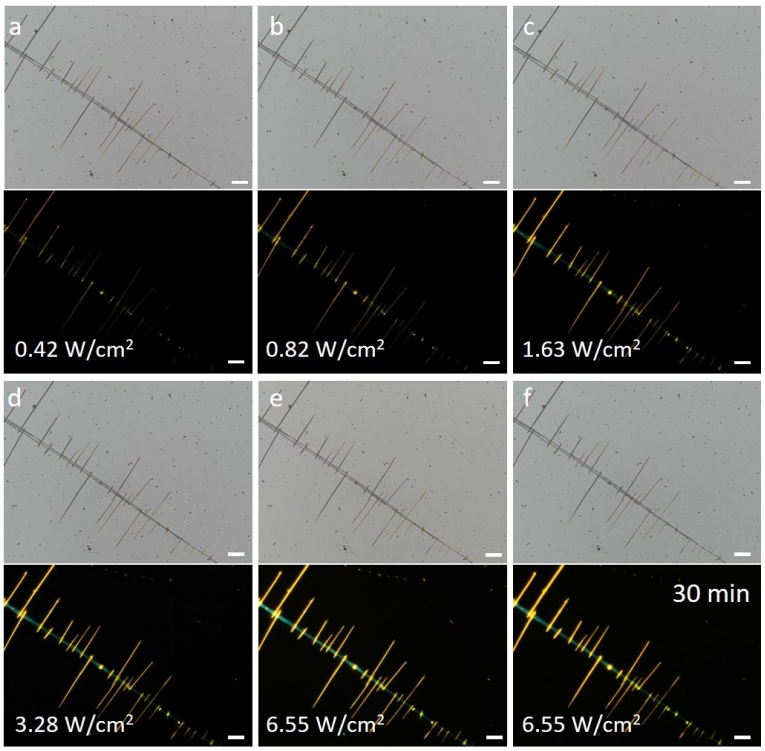

Figure S6. The stability of the M-BNwH under UV light (330-380 nm) irradiation with different power. (a-e) The bright field and fluorescent micrographs of M-BNwH irradiated by a UV excitation source with power of (a) 0.42 W/cm^2, (b) 0.82 W/cm^2, (c) 1.63 W/cm^2, (d) 3.28 W/cm^2 and (e) 6.55 W/cm^2, respectively. (f) The bright field and fluorescent micrographs of M-BNwH irradiated by light source with power of 6.55 W/cm^2 for 30 minutes. The scale bar is 10 μm.

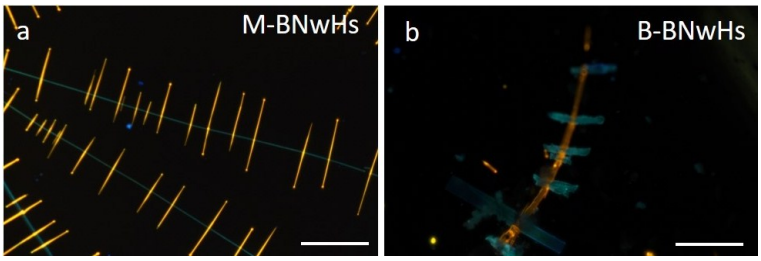

Figure S7. The fluorescent micrographs for organic heterostructures of (a) M-BNwHs and (b) B-BNwH after exposed in air for half a year. The scale bar is 10 μm.

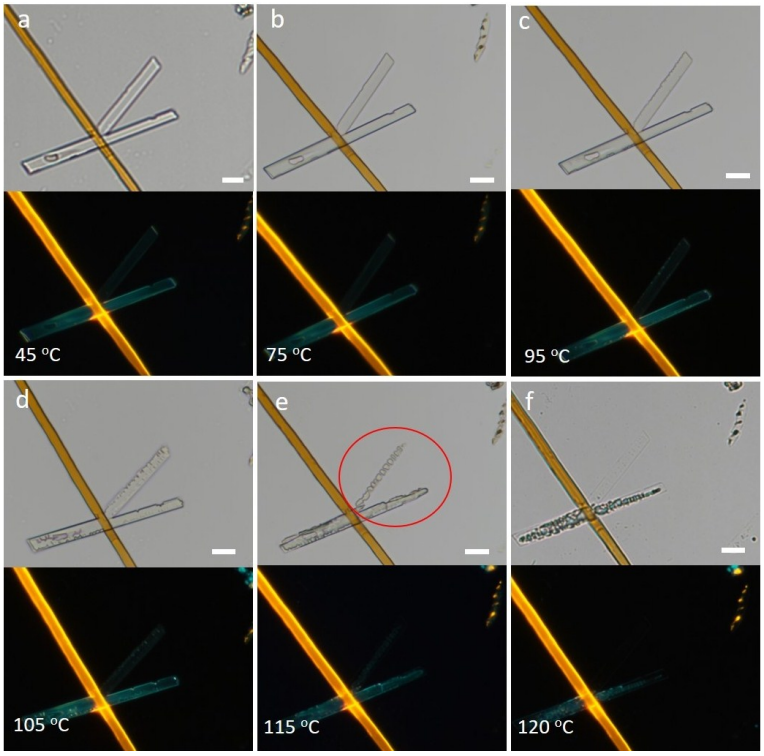

Figure S8. The thermal stability of the B-BNwH. The bright field and fluorescent micrographs of B-BNwH after thermal treatment at (a) 45 °C, (b) 75 °C, (c) 95 °C, (d) 105 °C, (e) 115 °C and (f) 120 °C, respectively. The scale bar is 10 μm.

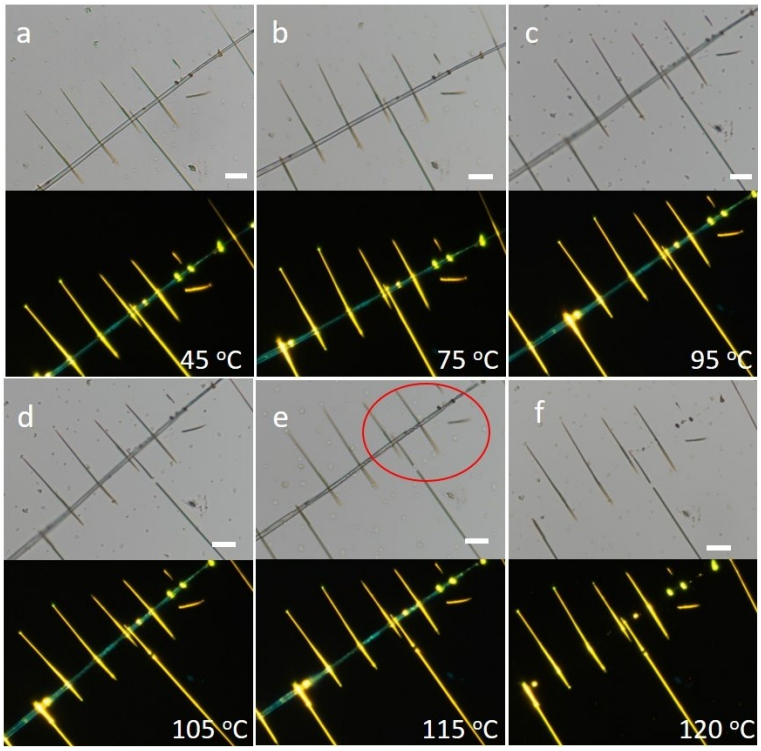

Figure S9. The thermal stability of the M-BNwH. The bright field and fluorescent micrographs of M-BNwH after thermal treatment at (a) 45 °C, (b) 75 °C, (c) 95 °C, (d) 105 °C, (e) 115 °C and (f) 120 °C, respectively. The scale bar is 10 μm.

7. Fluorescence micrographs of MCzT and BPEA nanostructures excited by UV (330-380 nm) and green light (510-560 nm).

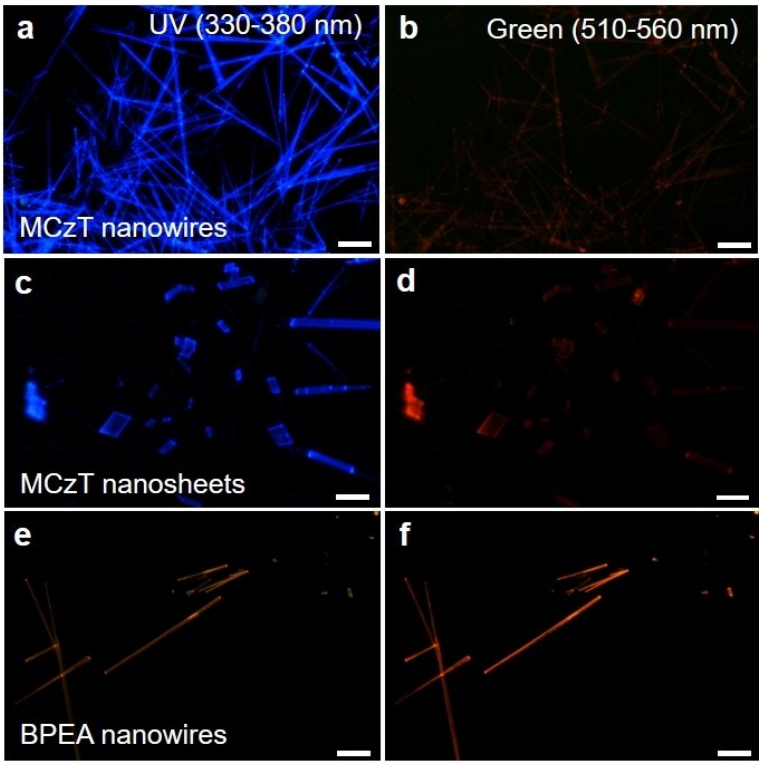

Figure S10. The fluorescence micrography images of MCzT and BPEA nanostructures excited by UV light (330-380 nm) and green light (510-560 nm). (a, b) The images of 1D MCzT nanowires excited by UV and green light. (c, d) The images of 2D MCzT nanosheets excited by UV and green light. (e, f) The images of BPEA nanowires excited by UV and green light. The scale bars of (a, b, e, f) are 25 μm. The scale bars of (c, d) are 10 μm.

8. The dual anti-counterfeiting application of M-BNwHs.

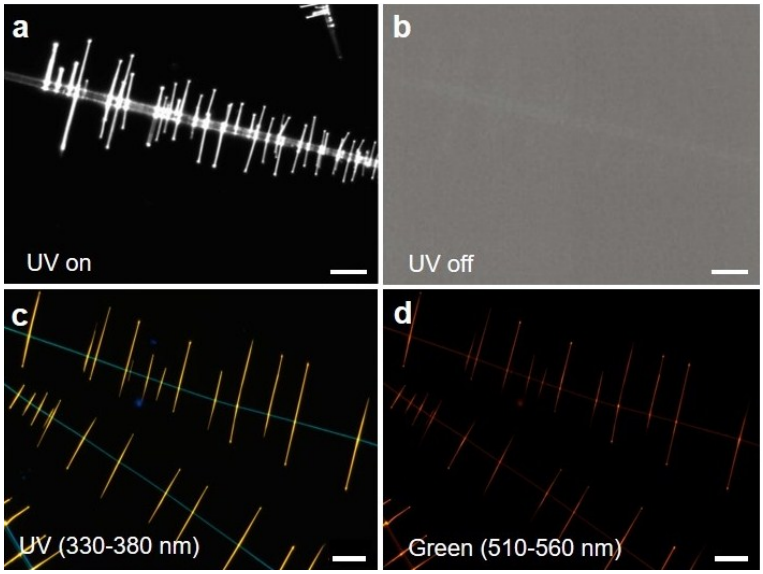

Figure S11. The dual anti-counterfeiting application of M-BNwHs. (a) The micrography images of M-BNwHs excited by UV light (330-380 nm). (b) The black-white micrography images of M-BNwHs taken at 0.5 s after turning off the excitation. (c, d) The images of M-BNwHs excited by UV light (330-380 nm) and green light (510-560 nm). The scale bar is 10 μm.

9. SEM images of BPEA, MCzT, M-BNwHs and B-BNwHs.

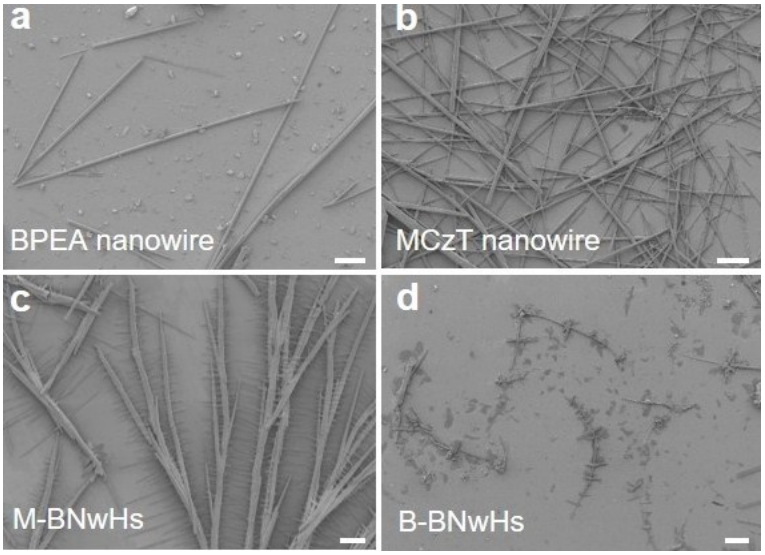

Figure S12. Typical SEM images of (a) BPEA nanowires, (b) MCzT nanowires, (c) M-BNwHs, (d) B-BNwHs. The scale bars of (a, d) are 50 μm. The scale bars of (b, c) are 10 μm.

10. Unit cell parameters of MCzT and BPEA crystals.

Table S1. Unit cell parameters of MCzT and BPEA crystals.

Molecule	MCzT	BPEA
Formula	$C_{17}H_{14}N_4O_2$	$C_{30}H_{18}$
Space Group	C 2/c	P b c n
Cell Lengths (Å)	*a* 9.772(2) *b* 20.088(5) *c* 7.2777(18)	*a* 24.305(4) *b* 11.512(1) *c* 7.099(1)
Cell Angeles (°)	*α* 90 *β* 91.758 *γ* 90	*α* 90 *β* 90 *γ* 90

11. The quantum yields of M-BNwHs and B-BNwHs.

Table S2. The quantum yields of M-BNwHs and B-BNwHs.

Compound	Quantum yields
M-BNwHs	56.9%
B-BNwHs	31.9%

12. Supporting videos.

SV1 and **SV2**. The co-assembly processes of M-BNwHs (SV1) and B-BNwHs (SV2). The supplementary videos were recorded by Nikon DS-Ri2 Microscope Camera under ambient conditions.